Appl. Phys. A 78, 531–536 (2004)
DOI: 10.1007/s00339-003-2454-4

Applied Physics A
Materials Science & Processing

F. PACHECO[1]
M. GONZÁLEZ[1]
A. MEDINA[2]
S. VELUMANI[3]
J.A. ASCENCIO[3,✉]

Structural analysis of cobalt titanate nanoparticles obtained by sol–gel process

[1] Universidad Popular Autónoma del Estado de Puebla, 21 sur 1103, Col. Santiago, Puebla, Pue., México
[2] Instituto de Metalurgia, Universidad Michoacana de San Nicolas de Hidalgo, P.O. Box 52-B 58000, Morelia, Mich., México
[3] Programa de Ingeniería Molecular, Instituto Mexicano del Petróleo, Eje Central Lázaro Cárdenas No. 152, Col. San Bartolo Atepehuacan, D.F., México

Received: 20 October 2003/Accepted: 22 October 2003
Published online: 19 December 2003 •

ABSTRACT In this work we report the synthesis of nanocomposites based on nanoparticles of cobalt titanate and titanium dioxide in their anatase crystalline phase by a sol–gel process. The synthesized nanoparticles of titanate vary from 1 to 6 nm in size. They are embedded in the anatase matrix, and they were obtained from TiO_2 monoliths doped with Co^{2+}. The formation of cobalt titanate nanoparticles showed a linear dependence on the cobalt concentration. The cobalt titanate nanocrystals are very stable even at temperatures higher than 1000 °C. The crystalline structures of the samples were examined using high-resolution transmission electron microscopy and X-ray diffraction. Molecular simulation methods were utilized for a better understanding and for improving the analytical data interpretation of the experimental results.

PACS 61.16.Bg; 79.60.Jv; 61.46.+w; 61.50.Ah

1 Introduction

Metal oxide nanoparticles like titanium dioxide individually and doped with other metallic compounds have gained much importance due to their multifaceted applications, more specifically in catalysis, photocatalysis [1, 2] and in the development of electronic and photonic materials and devices [3]. The synthesis and use of nanostructures based on titanium dioxide has attracted the attention of many researchers in different fields, particularly when the structures are smaller than a few nanometers and the quantum size effects become significant. The initial formal works on semiconductor nanoparticles of quantum size during 1981 [4–6] triggered multifarious activity in this field of investigation. Most of the semiconductor materials, such as the II/IV or III/IV compounds, show a quantum confinement effect in the range of 1–20 nm [7, 8]. The TiO_2 nanoparticles exhibit a chemiluminescence behavior when the cluster size reaches around 20 nm [9]. Also, the $BaTiO_3$ structures show a transition from a ferroelectric phase to a nonferroelectric one when their size decreases to less than 100 nm [10, 11]. There are reports of nonlinear optical response in poly(p-phenylene-benzobisthiazole) layers embedded with TiO_2 layers in less than a 50-nm^2 area [12].

The synthesis of doped TiO_2 by a sol–gel process has been broadly studied. It is well known that impurities like cations in a TiO_2 gel allow the control of the anatase–rutile phase transition and the stabilization of the anatase phase at higher temperatures [13, 14]. In this way, it is also possible to obtain a wide variety of binary oxides with the formula $ATiO_3$ by sol–gel methods [15–19] or composites such as $NdAlO_3$ nanocrystals embedded in an Al_2O_3 matrix [20]. Furthermore, it has been reported that by combining sol–gel with methods of hydrolysis injection it is possible to synthesize binary oxide nanoparticles and to produce self-assembled arrays generating nanostructured superlattices [21]. The synthesis of mixed oxides obtained from TiO_2 is interesting because of the possible technological application of these compounds. Particularly, cobalt titanate ($CoTiO_3$) has an important impact in the production of semiconductor devices, since with this oxide it is possible to manufacture thin films of very high κ constant [22–24]. Besides, it is well known that TiO_2, in its anatase or rutile phase, is a dielectric material with a value of κ which is not easily reached by other metallic oxides, but still it has several disadvantages against SiO_2; hence the alternative is to combine the desirable properties of two or more oxides to eliminate the undesirable properties of each individual material [25].

In this work, we report the synthesis of cobalt titanate nanoparticles embedded in a titanium dioxide matrix by a sol–gel technique and the corresponding characterization of the composite in anatase phase. Structural characterization was carried out using X-ray diffraction in order to determine the crystalline phase at different concentrations and temperatures, while high-resolution transmission electron microscopy (HRTEM) was used to determine the structure and composition of local arrangements of crystalline grains and nanoparticles. Besides the analytical data, we used molecular and HRTEM simulation tools for a better understanding and a well-supported interpretation of the experimental results [26].

2 Experimental method

The cobalt-doped TiO_2 sols were synthesized by a sol–gel process as

✉ E-mail: ascencio@imp.mx

Sample	TIPO	Water	Isopropanol	$Co(NO_3)_2$	Acetic acid
03	1	2	20	0.03	3
06	1	2	20	0.06	3
08	1	2	20	0.08	3
09	1	2	20	0.09	3
10	1	2	20	0.10	3
12	1	2	20	0.12	3

TABLE 1 Summary of the solution (sol) compositions and reagents

reported in our earlier article [27]. Several different sols were prepared varying just the cobalt molar concentration as shown in Table 1, where the molar relationship is shown with regard to titanium isopropoxide (TIPO), for all the chemical reagents used.

The sols obtained were made as gel in air at room temperature for 6 months. Small monoliths were obtained from the cobalt-doped TiO_2 gels. After ageing them, the amorphous monoliths were thermally treated in air at 550 °C for 2 h, and the structural analysis was done using a Siemens D5000 X-ray diffractometer to identify the crystalline phases. The samples were pulverized to a fine powder and were mounted on a Cu grid with amorphous carbon as a support for transmission electron microscopy (TEM) analysis. The HRTEM images were obtained in a FEG FEI Tecnai TEM with an acceleration voltage of 200 kV, a spherical aberration of $C_s = 1$ mm and a point resolution of ≈ 1.6 Å. The HRTEM images were obtained in digital format using the camera inside the microscope, and the digital images were processed in both the real and Fourier spaces. This processing was used for filtering the corresponding frequencies for each phase in the sample; with this process the structure of the observed sample can be enhanced [28].

From the experimental data, models for each cluster were obtained by using the modules of Crystal Builder and the visualizer of Cerius [2] by Accelrys. The models were used to calculate the minimum-energy configuration for nanoparticles in each case and finally the obtained configurations were used to calculate HRTEM simulated images by using the SimulaTEM software developed by Gómez and Beltrán [29], which is based on the use of the multislice method. Both the experimental and theoretical data were compared in order to understand the behavior of the sol–gel-synthesized nanoparticles.

3 Results and discussion

Samples obtained by this technique are comparatively large and so it was possible to allocate similar samples for different characterizations. The first was to identify the crystalline phases present in the synthesized material, including an analysis at different temperatures that allowed us to study the thermal response based on the crystalline structures which are associated with the reflections in the diffractogram. In Fig. 1, an X-ray-diffraction (XRD) pattern for the samples with different concentrations is shown. From these XRD patterns it is possible to identify that, for the 0.03 cobalt molar concentration, just the anatase phase of TiO_2 is present, while for the other concentrations we were able to identify mixtures of anatase and cobalt titanate phases. As expected, it can be observed that the quantity of titanate increase significantly when the cobalt concentration increases in the sols.

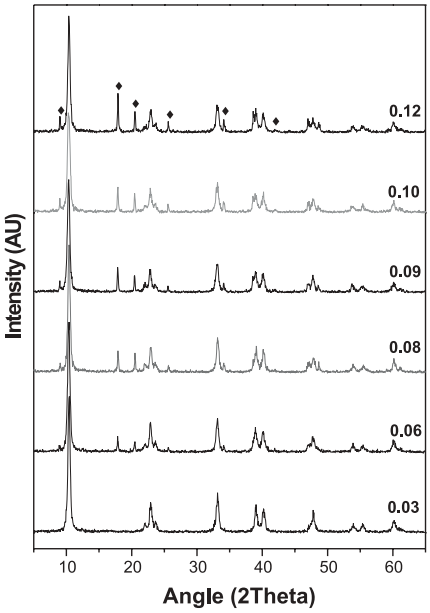

FIGURE 1 X-ray diffraction pattern sequence for cobalt doped TiO_2 for the 0.03, 0.06, 0.08, 0.09, 0.10 and 0.12 molar concentration. The corresponding pattern to 0.03 shows the typical spectrum of the anatase phase of TiO_2, while the other patterns present additional peaks that correspond to the cobalt titanate crystalline phase (♦)

The XRD pattern in Fig. 2 shows that the cobalt titanate oxide is stable even after thermal treatment up to 1100 °C and along with the $CoTiO_2$ peak we are able to identify the rutile TiO_2 phase. This becomes really important because the cobalt titanate suffers an intrinsic reduction at that temperature in bulk configuration, while in this case the cobalt titanate was found to remain stable.

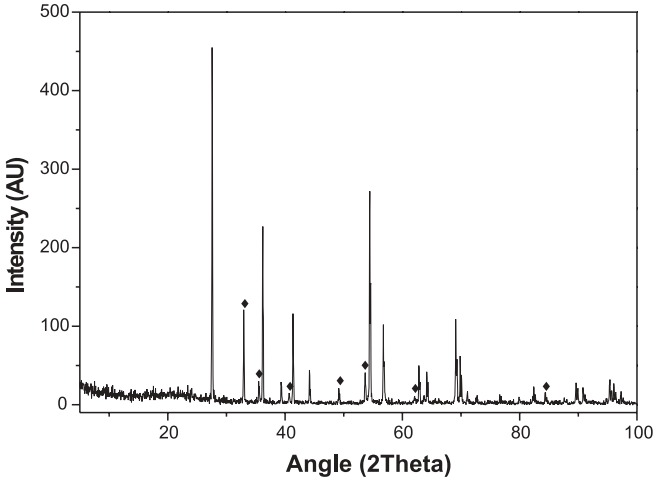

FIGURE 2 X-ray diffractogram of the sample 09 treated thermally at 1100 °C, the *marks* (♦) indicate the characteristic peaks of the cobalt titanate and the peaks with out marks indicate the characteristic peaks of the rutile TiO_2 crystal

Based on the XRD patterns it is possible to distinguish the existence of the different phases and, because of the small contribution, we needed to make smaller powder to be studied in the TEM. These samples were studied at the optimum contrast based on the Scherzer condition, where two or more phases can be distinguished even with small domains overlapped [28, 30, 31]. The conditions to get this effect are complicated and even more so in the case of small differences in the lattice parameters of the crystals, as in this case. Digital processing methods are used in order to improve the contrast and to extract the information from the HRTEM images.

In Fig. 3, a common HRTEM image of the sample (sample 09 described in Table 1) is shown. The lattice resolution can be observed clearly because the crystalline spacing is bigger than the resolution limit of the microscope. From the original micrograph (Fig. 3a), and its corresponding fast Fourier transform (FFT) (Fig. 3b), it is possible to identify the different lattices that correspond to different structures. With the help of frequency filtering, we can split the different signals, relating them to the crystalline parameters and the composition of the clusters. In Fig. 3c–e decomposition images are shown, selecting the masks that are shown below each image. In the case of selecting the external dots (first image), this allows us to obtain just the contrast produced by the smallest distances, the second image corresponds to the dots at an intermediate distance to the center and the last image corresponds to the smallest frequencies or the biggest lattice spacing; however the use of this method allows us to recognize that there are two main structures and the last image must correspond to Moiré fringes, produced by the overlapping of these phases.

In the image of Fig. 3c one of the clusters shows the spacings of 2.38 and 2.33 Å that correspond to the (004) and (112) planes' distances respectively for the TiO_2 anatase phase; besides, the measured distances of 2.22 and 2.53 Å match the (110) and (111) planes; and finally the distance of 3.72Å obtained in Fig. 3d corresponds to the spacing between the (012) planes. With these values of the distances in the clusters, it is possible to identify the anatase phase and the corresponding phase for cobalt titanate oxide, which coincide with the observed phases in the XRD patterns. However, the contrasts of these particles are quite similar, and the use of theoretical support helps to a better interpretation; then the calculation of HRTEM images from models of the structures observed in the XRD becomes quite important.

In Fig. 4, the simulated images for the two cases of anatase (a) and cobalt titanate oxide (b) are shown, and they allow identifying the significant differences between the produced contrasts for each case. In order to help a better understanding, the structures were rotated in steps of 15° over both *a* and *b* axes, producing a kind of plateau; besides the images, for the original and 90° orientations the models are also included. From the simulated data, it is possible to identify several parameters and details to distinguish the presence of these crystals in the studied sample, for instance: in Fig. 4a, the anatase crystal produces contrasts of dots not forming perfect squares (15°, 15°) and also there can be found hexagons of two types; one of them is observed in the (30°,

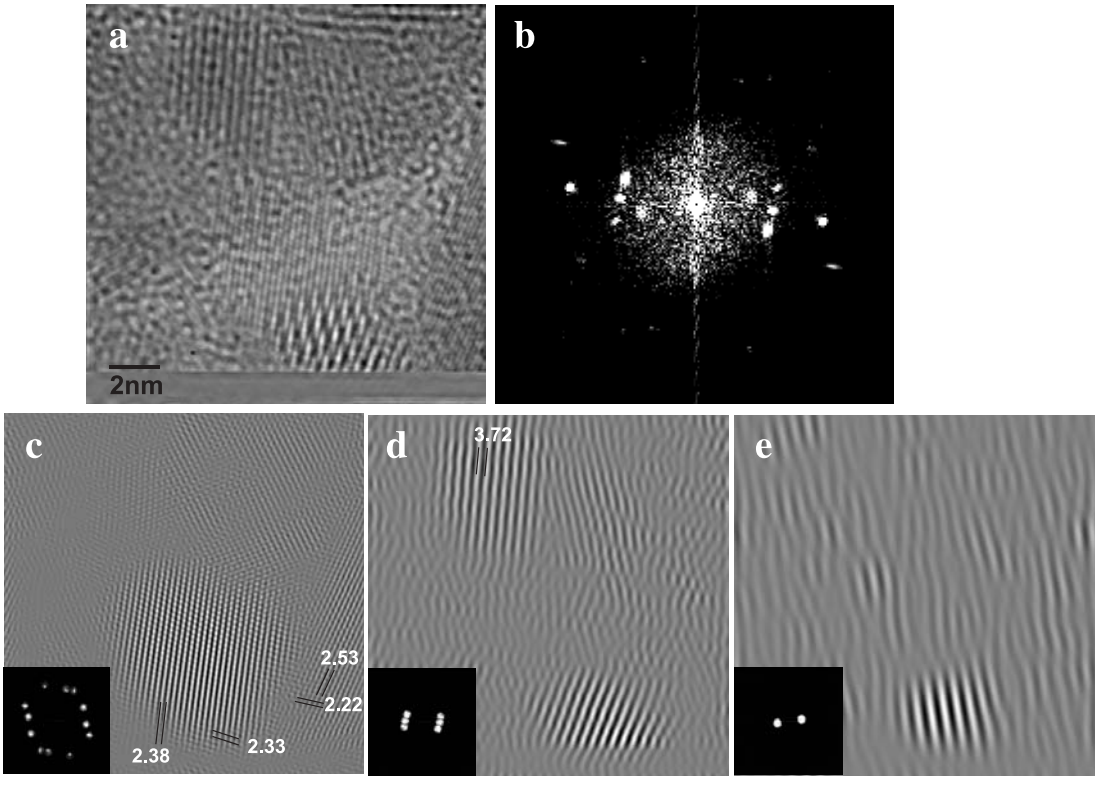

FIGURE 3 HREM analysis of a common structure in the sample. The HRTEM image (**a**) is shown besides its corresponding FFT (**b**) and three different filtered images for different frequencies. The interplanar distances are also shown for clarity

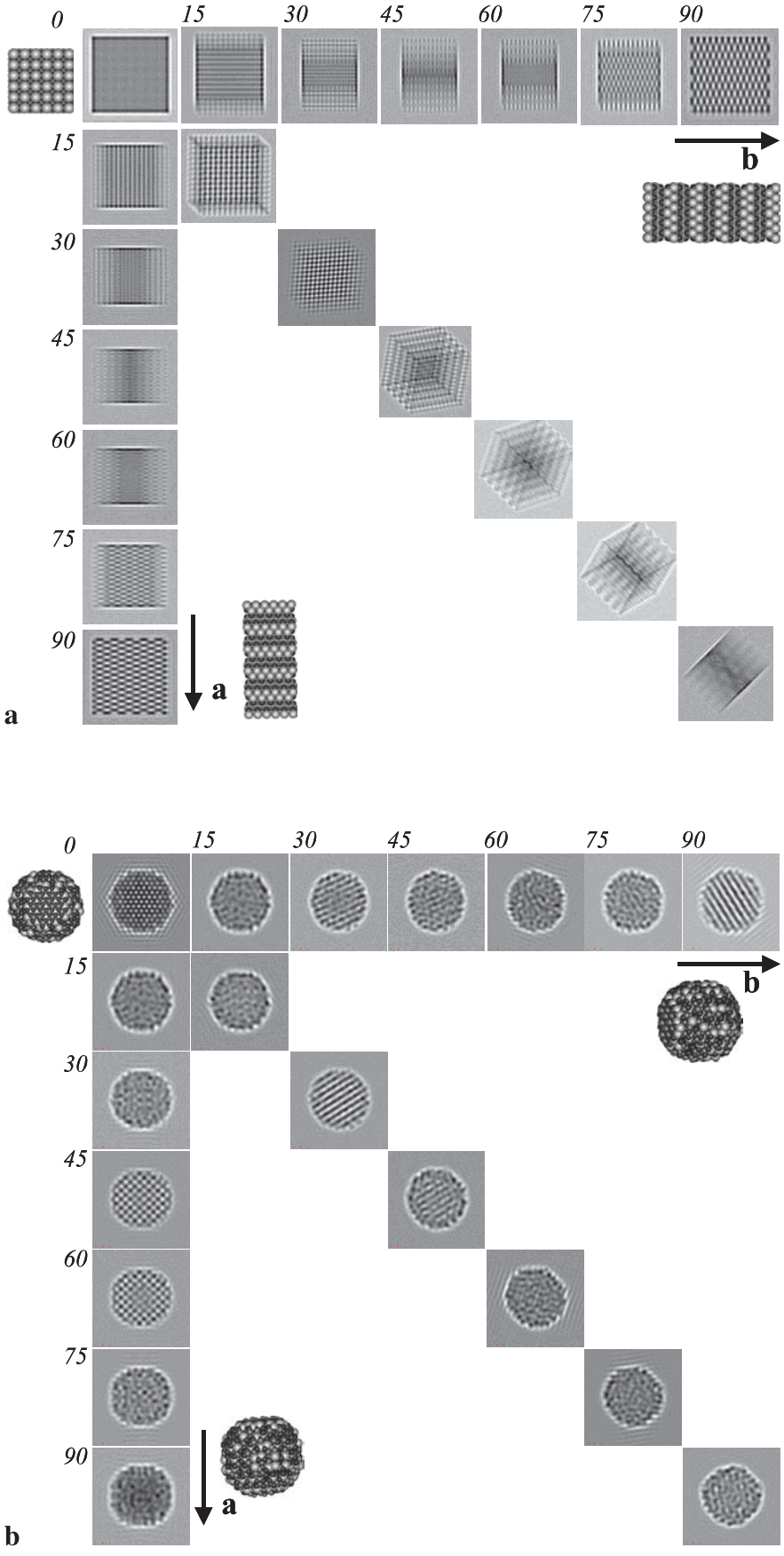

FIGURE 4 HRTEM images calculated for each 15 °C, for models of **a** anatase and **b** cobalt titanate oxide

30°) image, where the hexagons can be clearly identified and also in the images of (90°, 0°) and (0°, 90°), where the hexagons are formed by elongated dots; also a really interesting contrast is obtained when the overlapping of the planes produces empty zones and longer distances between lines as in the case of (45°, 45°), (60°, 60°) and (75°, 75°). Besides, in Fig. 4b, the contrast produced by the model of clusters only generates dot contrast in the (0°, 0°) images, while lines appear in several images, even producing squares in the (0°, 45°) and (0°, 60°) images. In this last model, many images produce no recognizable contrast, which is produced by the internal atoms that truncate lines depending on the orientation, until they show amorphous patterns in several rotations.

Even when in the different calculated models, the produced images have several similar details and planar spacing; the (1, 1, 1)-plane families produce different contrasts for the different crystals, for instance in the anatase case these kinds of planes are quite difficult to identify with the microscope used because of the internal atoms and the scattering produced by the Ti atoms, which is stronger than the oxygen atoms and generates a zigzag-like contrast as observed in the (45°, 45°) corresponding image. Finally, in the corresponding calculations for cobalt titanate these planes appear to be not fully flat or partially interrupted because of the periodicity between the Ti, Co and O atoms that produces significant changes in the electron-scattering proportion. Besides the (1, 1, 1) planes, the (2, 0, 0)-like ones contribute to the dot contrast, producing squares and hexagons in different images, which are easier to distinguish.

With the help of this imaging system and the corresponding lattice measurements, more than 100 HRTEM micrographs were studied in order to distinguish the size distribution of the produced clusters, obtaining a distribution shown in Fig. 5, where the size distributions for both kinds of structures (anatase and cobalt titanate oxide) are studied. In the obtained plot, there is a clear distribution of nanoparticles in the range of 1 to 7 nanometers for both kinds of structures. The total cobalt titanate oxide nanoparticles are obtained from 2 to 6 nanometers with the great-

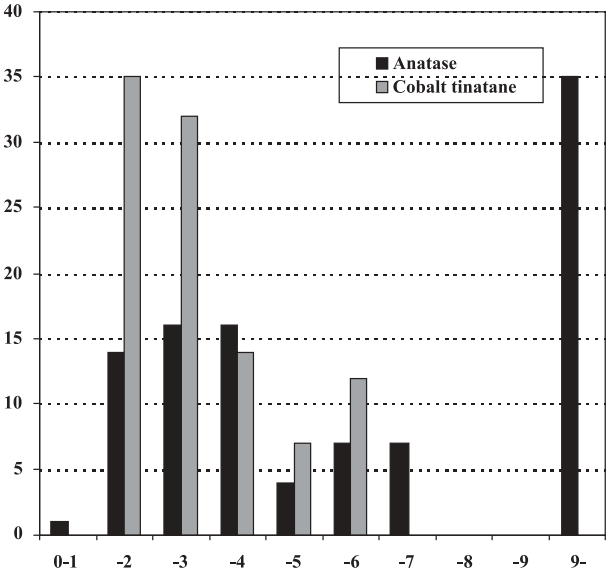

FIGURE 5 Size distribution plot for the nanoparticles identified in the samples

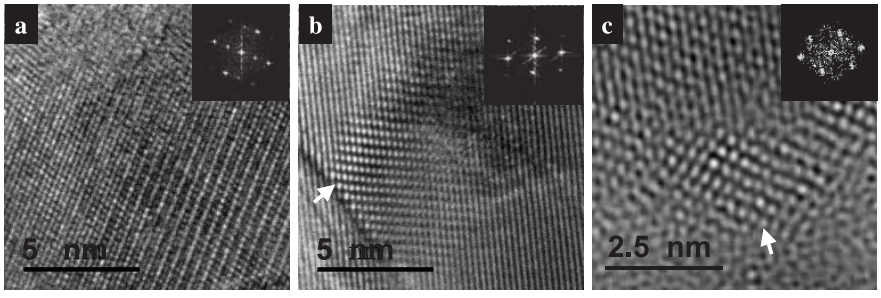

FIGURE 6 Examples of HRTEM images for the cases of **a** big anatase structures, **b** nanoparticles of anatase and **c** nanoparticles of cobalt titanate oxide. The nanoparticles are denoted using *white arrows*

est quantity between 2 and 3 nm, with more than 66%. However, in the case of anatase, the greatest quantity of observed structures is bigger than 9 nm, which must correspond to the bigger materials that form the matrix and the bigger crystals.

From this study there is observable the formation of nanoparticles of both materials; however the bigger quantity of anatase is mainly evidenced in the matrix and the bigger particles. But the cobalt titanate oxide is formed in small clusters which tend to be rounded and a big quantity is nearly in the range of quantum dots, which must involve an important improvement in the properties, mainly electronic behavior that is significantly affected by the size at this scale.

The structures of these particles are based on the crystalline origin and tend to be round in shape, because of the minimal surface-energy condition and property of the clusters at this scale. As can be observed in Fig. 6, large areas of the samples are covered by the anatase phase, which tends to grow into big crystals (Fig. 6a). Besides this behavior we can identify that the small grains of anatase produced are immersed in the matrix of the same phase. In Fig. 6b there is marked a cluster of 4 nm in diameter; the formation of these clusters must be caused by the lower energy on the surface, which also induces deformation of the external atoms as can be observed in the micrograph [31]. Similarly, the production of cobalt titanate oxide clusters is identified with contrast similar to that calculated, but with a smaller size; in Fig. 6c a 2-nm cluster is shown with the hexagonal array that could be identified in the 001 orientation. In the three images, the phase was distinguished using the corresponding lattice spacing for each material.

4 Conclusions

In this work we have proved the possibility of obtaining a nanocomposite based on the production of nanoparticles of titanium oxides in anatase phase but also cobalt titanate oxide clusters in different sizes from 2 to 6 nm by using a sol–gel method. The samples were studied and characterized by XRD and HRTEM, which allowed the understanding of the size distribution and the corresponding local structures. Besides the direct observation a full digital process based on frequency filtering and simulation tools is shown for obtaining distinguishable parameters of two different phases of crystals with near-lattice parameters. The digital and HRTEM simulation methods allowed distinguishing the different materials, even when they are overlapped, using local information with the small differences of contrast and lattice spacing that implies a complicated problem that is not possible to be solved by mean of the X-ray diffractogram patterns. This work demonstrates that the sol–gel method allows synthesizing small nanoparticles of cobalt titanate embedded in a matrix of anatase and that the produced structures are mainly dominated by the crystalline phase in the bulk scale; however a few local sections were evidenced where deformation on the periodicity is made in order to reduce the surface energy when the smallest clusters are formed.

REFERENCES

1 K. Rajeshwar, C.R. Chenthamarakshan, S. Goering, M. Djukic: Appl. Chem. **73**, 1849 (2001)
2 G. Alhakimi, L.H. Studnickib, M. Al-Ghazalic: J. Photochem. Photobiol. A: Chem. **154**, 219 (2003)
3 H.S. Nalwa (ed.): *Handbook of Advanced Electronic and Photonic Materials and Devices* (Academic Press, San Diego 2001)
4 K.E. Drexler: Proc. Natl. Acad. Sci. **78**, 5275 (1981)
5 G.C. Papavassiliou: J. Solid State Chem. **40**, 30 (1981)
6 J.A.A.J. Perenboom, P. Wyder, F. Meier: *Electronic Properties of Small Particles* (North-Holland, Amsterdam 1981)
7 K. Rajeshwar, N.R. Tacconi, C.R. Chenthamarakshan: Chem. Mater. **13**, 2765 (2001)
8 T. Trindade, P. O'Brien, N.L. Pickett: J. Mater. Chem. **13**, 3843 (2001)
9 Y. Zhu, J. Shi, Z. Shang, C. Zhang, X. Shang: Anal. Chem. **74**, 120 (2001)
10 W.Y. Shih, A. Aksay: Phys. Rev. B **50**, 15 575 (1994)
11 T. Lee, I.A. Aksay: J. Cryst. Growth **1**, 401 (2001)
12 G.L. Fisher, R.W. Boyd, R.J. Gerh, S.A. Jenekhe, J.O. Osaheni, J.E. Sipe, L.A. Weller-Brophy: Phys. Rev. Lett. **74**, 10 (1995)

13 R. Rodríguez-Talavera, S. Vargas, R. Arroyo-Murillo, R. Montiel-Campos, E. Haro-Ponia towski: J. Mater. Res. **12**, 439 (1997)
14 S. Vargas, R. Arroyo, E. Haro, R. Rodríguez: J. Mater. Res. **14**, 3932 (1999)
15 D. Bersani, P.P. Lotteci, A. Montenero, S. Pigoni, G. Gnappi: J. Mater. Sci. **31**, 3153 (1996)
16 T. Gubert, U. Beck, H. Kleinke: J. Non-Cryst. Solids **196**, 150 (1996)
17 D. Bersani, P.P. Lotteci, M. Canali, A. Montenero, G. Gnappi: J. of Sol–Gel Sc. Techn. **8**, 337 (1997)
18 D. Bersani, P.P. Lotteci, T. López, X. Ding: J. of Sol–Gel Sc. Techn. **13**, 849 (1998)
19 J.A. Wang, R. Limas-Ballesteros, T. López, A. Moreno, R. Gómez, O. Novaro, X. Bokhimi: J. Phys. Chem. B **105**, 9692 (2001)
20 T. Ming Pan, T. Fu Lei, T. Sheng Chao, K. Lih Chang, K. Chien Hsieh: Electrochem. Solid-State Lett. **3**, 433 (2002)
21 S. O'Brien, L. Brus, C.B. Murray: J. Am. Chem. Soc. **123**, 12 085 (2001)
22 T. Ming Pan, T. Fu Lei, T. Sheng Chao: Appl. Phys. Lett. **78**, 433 (2001)
23 S. Mathur, M. Veith, H. Shen, S. Hüfner, M.H. Jilavi: Chem. Mater. **14**, 568 (2002)
24 T. Ming Pan, T. Fu Lei, T. Sheng Chao: J. Appl. Phys. **89**, 3447 (2001)
25 G.D. Wilk, R.M. Wallace, J.M. Anthony: J. Appl. Phys. **89**, 5243 (2001)
26 M. José-Yacamán, C. Zorrilla, J.A. Ascencio, G. Mondragón, J. Reyes-Gasca: Mater. Trans. JIM **40**, 141 (1999)
27 F. Pacheco, R. Palomino, G. Martínez, A. Mendoza, R. Rodríguez, V. Castaño: Appl. Opt. **37**, 1867 (1998)
28 M. José-Yacamán, J.A. Ascencio: 'Electron Microscopy Techniques Applied to Nanostructured Materials and Ancient Materials'. In: *The Handbook of Nanostructured Materials and Nanotechnology*, ed. by H.S. Nalwa (Academic Press, San Diego 1999)
29 A. Gómez, L. Beltrán: Software SimulaTEM. Available at http://www.ifunam.unam.mx (2000)
30 I. Arvanitidis, A. Kapilashrami, D. Fichen, S. Seertharaman: J. Mater. Res. **15**, 338 (2000)
31 M. José-Yacamán, S. Tehuacanero, C. Zorrilla, J.A. Ascencio, A. Gómez: Nanostruct. Mater. **10**, 1 (1998)